Bibliographical reference

Modeling of Lossy Inductance in Moving-Coil Loudspeakers, Xiao-Peng Kong, Finn Agerkvist and Xin-Wu Zeng, Acta Acustica **vol. 101** (Number 3), 2015, pp. 650-656

DOI

https://doi.org/10.3813/AAA.918860

Acta Acustica united with Acustica
Vol. 101 (2015) 650 – 656

DOI 10.3813/AAA.918860

Modeling of Lossy Inductance in Moving-Coil Loudspeakers

Xiao-Peng Kong[1)], Finn Agerkvist[2)], Xin-Wu Zeng[1)]

[1)] College of Opto-Electronic Science and Engineering, National University of Defense Technology, Changsha 410073, P. R. China. kong@nudt.edu.cn

[2)] Acoustic Technology, DTU-Elektro, Technical University of Denmark, 2800 Kgs. Lyngby, Denmark

Summary

The electrical impedance of moving-coil loudspeakers is dominated by the lossy inductance in high frequency range. Using the equivalent electrical circuit method, a new model for the lossy inductance based on separate functions for the magnitude and phase of the impedance is presented. The electrical impedances of five loudspeakers were measured by Klippel LPM analyzer, and the model parameters were identified by fitting the measured impedance curve. The obtained accuracy was evaluated with respect to the simplicity of different models. The results show that, this new model agrees well with the measured electrical impedance, and gives an accurate prediction of the lossy inductance varying with frequencies, especially for the frequency dependent phase. Additionally, there are just three parameters in this new model, which gives simple and rapid parameter identification.

PACS no. 43.38.Ja, 81.70.Ex, 84.37.+q

1. Introduction

A moving-coil loudspeaker consists of a suspended diaphragm with an attached voice coil, positioned in a permanent magnetic field. The current flowing in the voice coil wire produces a magnetic field, and the magnetic field circulating the wire induces eddy currents in the conductive center pole, resulting in inductance losses. It has been frequently observed that the inductive rise of the voice coil is closer to +3 dB per octave, and not +6 dB as expected for an ideal inductor [1]. Only a simple inductor doesn't capture the inductance losses, therefore the lossy inductance Z_L is introduced by different fitting models. For small-signal excitation, a loudspeaker can be modeled as an equivalent electrical circuit in Figure 1 via four parameters (R_e, R_{es}, C_{mes} and L_{ces}) and one frequency dependent lossy inductance Z_L.

The accuracy and the simplicity are two basic qualities for fitting models. Accuracy means that the model should predict the values in good correspondences with experiments, and simplicity makes the fitting process or parameter identification easily and quickly. The first model of Z_L was presented by Vanderkooy [2], wherein the effect was illustrated as a semi-inductance, which is the function of the square-root of angular frequency. Nevertheless, the experiment data show that this model fails to predict the electrical impedance of many drivers in high frequency range [3]. Wright modeled Z_L by two separate weighed power functions in angular frequency for both the real part and the imaginary part [3]. Since the Wright model is not bounded to be minimum phase and not composed from a system of lumped electrical elements it may be deceived by measurement artifacts when used to represent a measured curve [4]. Leach introduced a variable exponent to an angular frequency variable [5] and Thiele-Small parameters can be easily acquired by this model since there are only two parameters. Unfortunately, both the Wright model and the Leach model cannot be directly realized as an analogue or digital systems. The L_2R_2 model as used in the Klippel system [6] introduces a series inductance connected to the second inductance shunted by resistance. Because it can be directly realized in nonlinear differential equations, it has been mostly used in simulating the nonlinear behaviors of loudspeakers [7]. However, it is only valid for a restricted frequency range [1, 8]. Thorborg et al incorporated Vanderkooy semi-inductance into the equivalent electrical circuit for modeling Z_L [1, 9]. This model can be applied to most of the electrodynamics' transducers, and it is closer related to the physics of the electrodynamic speakers [10, 11]. However, there are five parameters in this model, resulting in an increased complexity of fitting procedure. The modeling of such lossy inductance is a challenge that has not been satisfactory coped with until today, and the aim of this paper is to improve the accuracy without introducing many more parameters.

The separated power function (SPF) model was presented by using two power functions in angular frequency for fitting the magnitude part and the phase part of lossy inductance separately. Five moving-coil loudspeakers without ac-shorting devices [1] were tested by Klippel LPM

Received 01 July 2014,
accepted 13 December 2014.

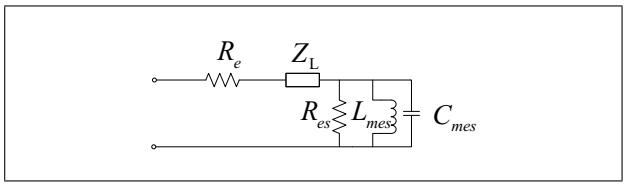

Figure 1. Equivalent voice coil circuit.

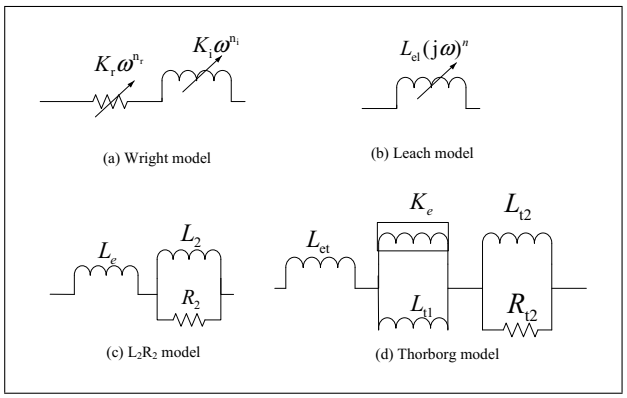

Figure 2. Equivalent circuits of fitting models.

analyzer under small signal input voltage. The SPF model with the other four classical models- Wright model, Leach model, L_2R_2 model and Thorborg model were evaluated by fitting the measured electrical impedance curve. The model accuracy was investigated by comparing the fitting results with the measured data, and the simplicity was analyzed by comparing the number of model parameters.

2. Fitting models

As shown in Figure 1, when studying the lossy inductance of voice coil, it is assumed that the series resistance has been treated as a separate element [10]. Figure 2 shows the equivalent circuits of the main four models in frequency domain (ω is angular frequency, j is the complex operator, i.e. $j^2 = -1$). All the fitting models are valid only for small signal input.

2.1. Wright model

There are four parameters in the Wright model (Figure 2a), K_r, n_r for the resistance part, and K_i, n_i for the reactance part, then the $Z_L(j\omega)$ becomes

$$\begin{aligned} Z_L(j\omega) &= K_r\omega^{n_r} + K_i\omega^{n_i} = Z_{LW}(\omega)e^{j\theta_W(\omega)}, \\ Z_{LW}(\omega) &= \sqrt{K_r^2\omega^{2n_r} + K_i^2\omega^{2n_i}}, \\ \theta_W(\omega) &= \omega^{n_i-n_r}(K_i/K_r). \end{aligned} \tag{1}$$

2.2. Leach model

Only two parameters were presented in the Leach model (Figure 2b), a constant inductance L_{el} and a variable exponent n,

$$\begin{aligned} Z_L(j\omega) &= L_{el}(j\omega)^n = L_{el}\omega^n e^{j\theta_L}, \\ \theta_L(\omega) &= n\pi/2, \quad 0 < n < 1. \end{aligned} \tag{2}$$

Studies show that the exponent parameter n lies in the range from 0.6 to 0.7, and that drivers having lower values of n usually have higher values of L_{el} [5]. Fitting parameters can be easily acquired by Leach model because it has only two parameters.

2.3. L_2R_2 model

As be depicted by Figure 2c, the L_2R_2 model introduces a series inductance L_e connected to the second inductance L_2 paralleled with resistance R_2. There are three parameters in $Z_L(j\omega)$,

$$Z_L(j\omega) = j\omega + \frac{j\omega L_2 R_2}{j\omega L_2 + R_2} = Z_{LK}(\omega)e^{j\theta_K(\omega)}, \tag{3a}$$

$$\begin{aligned} Z_{LK}(\omega) &= \sqrt{a_K^2 + b_K^2}, \\ \theta_K(\omega) &= \arctan\left(b_L/a_K\right), \\ a_K &= \omega^2 L_2^2 R_2/\left(L_2^2 + R_2^2\omega^2\right), \\ b_K &= \omega L_e + \omega L_2 R_2^2/\left(L_2^2 + R_2^2\omega^2\right). \end{aligned} \tag{3b, 3c}$$

2.4. Thorborgmodel

Figure 2d shows the Thorborg model, which uses a semi-inductance K_e to describe eddy currents and skin effect in the pole structures. $Z_L(j\omega)$ follows as

$$\begin{aligned} Z_L(j\omega) &= j\omega L_{et} + \frac{j\omega L_{t1}\sqrt{j\omega}K_e}{j\omega L_{t1} + \sqrt{j\omega}K_e} + \frac{j\omega L_{t2}R_{t2}}{j\omega L_{t2} + R_{t2}} \\ &= Z_{LT}(\omega)e^{j\theta_T(\omega)}, \end{aligned} \tag{4a}$$

$$\begin{aligned} Z_{LT}(\omega) &= \sqrt{a_T^2 + b_T^2}, \\ \theta_T(\omega) &= \arctan\left(b_T/a_T\right), \\ a_T &= A_1\omega^3 + A_2\omega \\ &\quad + A_3\sqrt{\omega}\left(A_4\omega^3 + A_5\omega^2 + A_6\omega + A_7\right), \\ b_T &= B_1\omega^4 + B_2\omega^2 \\ &\quad + A_3\sqrt{\omega}\left(A_4\omega^3 - A_5\omega^2 + A_6\omega - A_7\right), \\ A_1 &= L_{t2}^2 L_{t1}^3\left(L_{t2}R_{t2} - K_e\right), \\ A_2 &= L_{t2}^2 K_e^4 R_{t2} - K_e L_{t1}^3 R_{t2}^2, \\ A_3 &= 1/\sqrt{2}K_e L_{t1}^2, \quad A_4 = L_{t2}^2 L_{t1}^2, \\ A_5 &= L_{t2}^2 K_e^2, \quad A_6 = \omega L_{t1}^2 R_{t2}^2, \\ A_7 &= K_e^2 R_{t2}^2, \quad B_1 = \omega^4 L_{t2}^2 L_{t1}^4, \\ B_2 &= L_{t1}^4 R_{t2}^2 L_{et} + L_{t2}^2 K_3^4 + L_{t2}^2 K_e^4 L_{t1}. \end{aligned} \tag{4b, 4c}$$

2.5. SPF model

Measurements did by Bowler *et al.* show that $Z_L(j\omega)$ varies with frequencies (shown by Figures 5–7 in [12]). These measurements were made with the coil encircling a steel cylinder, in conventional loudspeaker metal work, *et al.* Figure 3 re-plots these measured $Z_L(j\omega)$ in [12] with one normal woofer measured by Klippel analyzer system. It shows that the magnitude part varies as positive power function in frequency, and the phase part decreases with

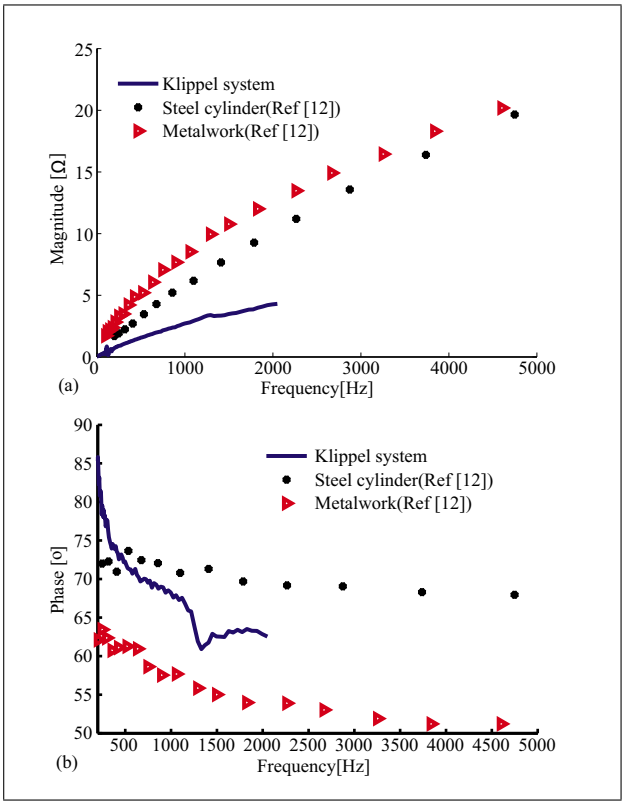

Figure 3. The measured lossy inductance. (a) magnitude (b) phase. The curves of steel cylinder and metalwork were reploted in form of magnitude and phase, instead of reactance and resistance shown by Figure 5 and Figure 7 in [12].

increasing frequency. It should be point out that the phase approached 90 degree at very low frequencies, $Z_L(\mathrm{j}\omega)$ behaves like an ideal inductance. This property corresponds to the observation that the eddy currents are frequency dependent and will vanish at very low frequencies [4]. Therefore, two different power functions in angular frequency were employed to predict the lossy inductance in form of magnitude and the phase. Then $Z_L(\mathrm{j}\omega)$ gives by only three parameters,

$$Z_L(\mathrm{j}\omega) = L_{ex}\omega^p \mathrm{e}^{\mathrm{j}\theta(\omega)}, \quad \theta(\omega) = \frac{\pi}{2}\omega^{-q}, \qquad (5)$$
$$0 < p < 1, \quad 0 < q < 1.$$

It is noteworthy to say that the power functions of lossy inductance can be described by fractional derivatives [8, 13]. For a lossy inductor, the electrical properties are described by the following fractional differential equations, $E(t) = L_e \mathrm{d}^\alpha i(t)/\mathrm{d}t^\alpha$ (where $0 < \alpha < 1$), and the fractional derivation $\mathrm{d}^\alpha/\mathrm{d}t^\alpha$ is defined as [14],

$$\frac{\mathrm{d}^\alpha f(t)}{\mathrm{d}t^\alpha} = {}_C D^\alpha i(t) = \frac{1}{\Gamma(m-\alpha)}\frac{\mathrm{d}}{\mathrm{d}t}\int_o^t \frac{f^{(m)}(\tau)}{(t-\tau)^{\alpha.m+1}}\,\mathrm{d}\tau, \quad (6)$$
$$m-1 < \alpha < m, \quad m \in \mathbf{N},$$

where $\Gamma(\cdot)$ is the gamma function and τ is an integration variable. By employing the fractional order Laplace operator of Caputo definition [15],

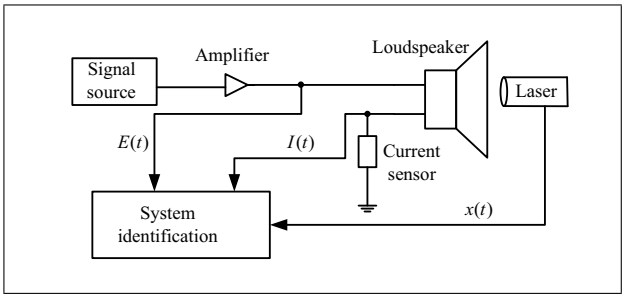

Figure 4. A sketch of the Klippel Analyzer setup circuit.

$$L\{{}_C D^\alpha f(t)\} = s^\alpha f(s) - \sum_{k=0}^{m-1} f^{(k)}(0), \quad s = \mathrm{j}\omega, \qquad (7)$$

if $f(t) = i(t)$ and $i(0) = 0$, then

$$L\{L_e {}_C D^\alpha i(t)\} = L_e s^\alpha i(s). \qquad (8)$$

Followed by Equatin (8), Leach model is described (Equation 2), and when $\alpha = 1/2$, then the inductor turns to be a semi-inductor which is widely used in Vanderkooy model.

3. Measurements and curve-fitting

3.1. Measurements of electrical impedance

Measurements were carried out on five speakers, two woofers, and three midrange speakers. Table I gives the specifications of tested loudspeakers.

3.1.1. Klippel analyzer set up

The Klippel analyzer has been widely used for identifying the loudspeaker parameters. A sketch of the Klippel Analyzer system is shown in Figure 4, where $E(t)$ is the input voltage, $I(t)$ is the output current, and $x(t)$ is the output diaphragmdisplacement measured by KEYENCE CO. LK-G32 laser. The laser is pointed at a small piece of reflective tape attached to the diaphragm. It uses triangulation to measure the distance from the laser to the diaphragm and thereby the displacement of the diaphragm. The system measures the loudspeaker parameters by means of system identification algorithm [16]. Linear parameters of loudspeakers can be measured from the *Linear Parameter Measurement* (LPM) in Klippel analyzer systems.

The influence of the room acoustics on the driver parameters can be neglected when having a normal room size (volume $> 30\,\mathrm{m}^3$) and keeping a distance of about one meter to the walls. A special mounting stand was used to fixate the driver in a vertical position with a laser displacement sensor placed in front of the diaphragm to measure the displacement, and loudspeakers were fixed in vertical position to avoid any offset in the displacement due to gravity. Simultaneous measurements of voltage, current and displacement were conducted on the five speakers.

Table I. Specifications of five tested loudspeakers.

Loudspeaker	Label	Type	Diameter [inch]	Resonance frequency [Hz]
L1	Peerless 831727	Woofer	10	30.1
L2	Scanspeaker25W/9565	Woofer	10	29.6
L3	Scanspeaker15W/8530	Midrange	5.25	39.1
L4	Peerless 850108	Midrange	5.25	111.5
L5	VifaP13WG-10-04	Midrange	5.25	116.5

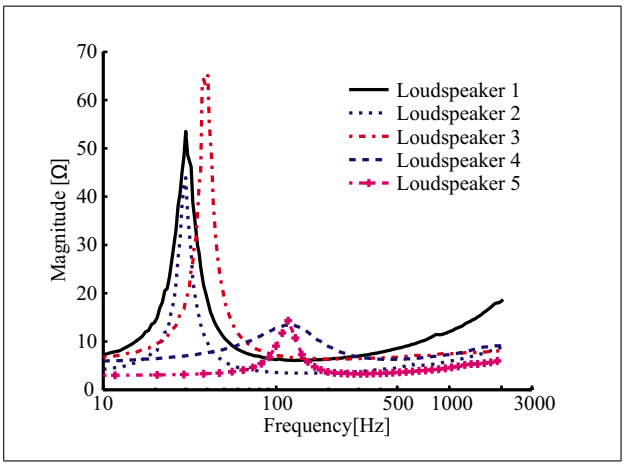

Figure 5. Measured electrical impedances magnitudes.

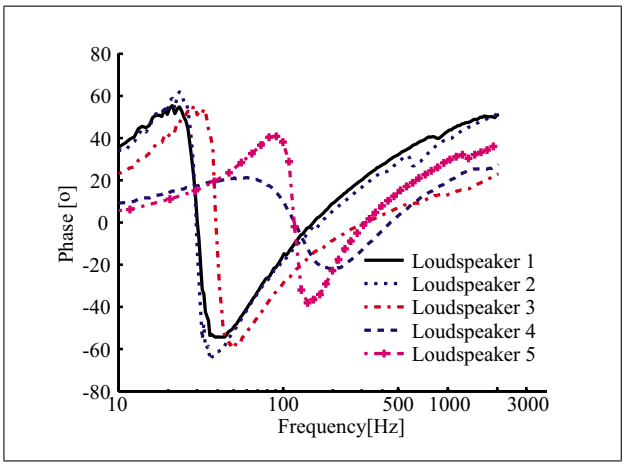

Figure 6. Measured electrical impedances phases.

3.1.2. Results

All measurements carried out under a RMS voltage level of 0.1 V in order to ensure all the speakers were working in the linear domain. The measured electrical impedance was calculated as a transfer function between the input voltage and the output current. Figure 5 and Figure 6 show the measured electrical impedance in form of magnitude and phase. These measurements also provided the raw spectra of the voltage, current and displacement, and these spectral data have been used for fitting $Z_L(\mathrm{j}\omega)$.

Figure 5 and Figure 6 show that at the resonance frequency the reactive part of the impedance switch sign from inductive to capacitive. In some of the operational range the impedance is largely resistive. Take loudspeaker 1 for instance, between 100 Hz to 500 Hz, the impedance varies only between 7 Ω and 8.5 Ω. These are typical values for speakers with a nominal impedance of 8 Ω. But at frequencies higher than 500 Hz, the impedance increases significantly as the inductance of the voice coil starts playing the main part of electrical impedance.

3.2. Curve-fitting

As the measured electrical impedances have been recorded, the investigated five models would fit to the measured data. If the model accurately predicts the lossy inductance, the electrical impedances should be very close to the measured data. The curve-fitting technology gives better model parameters, and in addition the possibility to separate the loudspeaker impedance into its electrical and motional impedance [11].

3.2.1. Fitting methods

The data fitting was done by minimizing the difference between the measured and calculated electrical impedance. The function *fminunc* in Matlab attempts to find a minimum of a cost function of several variables, starting at an initial estimate. The cost function κ to be minimized was defined as the relative deviation between the measured data and fitting results,

$$\kappa = \sum_i \left(\left| \frac{Z_{\mathrm{model}}(\mathrm{j}\omega_i) - Z_{\mathrm{meas}}(\mathrm{j}\omega_i)}{Z_{\mathrm{meas}}(\mathrm{j}\omega_i)} \right| \right), \quad (9)$$

$$Z_{\mathrm{model}}(\mathrm{j}\omega_i) = R_e + Z_L(\mathrm{j}\omega_i) + Z_{\mathrm{EM}}(\mathrm{j}\omega_i),$$

$$Z_{\mathrm{EM}}(\mathrm{j}\omega_i) = \left[\mathrm{j}\omega C_{\mathrm{mes}} + 1/(\mathrm{j}\omega L_{\mathrm{ces}} + 1/R_{\mathrm{es}}\right]^{-1}, \quad (10)$$

where $Z_{\mathrm{model}}(\mathrm{j}\omega)$ is the calculates electrical impedance and $Z_{\mathrm{meas}}(\mathrm{j}\omega)$ is the measured one. Equation (9) shows that in the cost function all the frequencies are weighted equally. Once the minimum κ was found, the model parameters were identified. The magnitude RMS error ζ_r and the phase RMS error ζ_i were used to make clear comparisons of different models,

$$\zeta_r(\%) = \sqrt{\frac{\sum_i \left(|Z_{\mathrm{model}}| - |Z_{\mathrm{meas}}|\right)^2}{\sum_i |Z_{\mathrm{meas}}|^2}} \cdot 100\%, \quad (11)$$

$$\zeta_i(^\circ) = \left| \frac{\sum_i \left[\arg(Z_{\mathrm{model}}) - \arg Z_{\mathrm{meas}})\right]^2}{N} \right|, \quad (12)$$

where N is the number of frequencies, and arg(.) is the function to calculate the phase (in degree) of variables.

Table II. Fitting errors.

Model	Wright		Leach		L_2R_2		Thorborg		SPF	
	ζ_r [%]	ζ_i [°]	ζ_r [%]	ζ_i [°]	ζ_r [%]	ζ_i [°]	ζ_r [%]	ζ_i [°]	ζ_r [%]	ζ_i [°]
L1	2.85	1.61	2.89	1.41	3.74	2.19	2.83	1.58	2.88	1.30
L2	3.98	1.61	4.01	1.45	4.19	1.47	3.50	1.47	3.51	1.45
L3	3.68	1.17	3.60	0.97	3.63	1.17	3.60	1.30	3.42	1.01
L4	3.21	1.23	2.51	0.91	3.78	1.03	2.96	1.32	2.62	0.89
L5	2.40	1.27	2.22	0.96	3.39	1.04	4.10	1.87	2.25	0.98

3.2.2. Fitting results

Table II shows the fitting errors ζ_r and ζ_i of all the five loudspeakers. They were also plotted in Figure 7. For all the five fitting models, the maximum of ζ_r is less than 4.5%, and the maximum of ζ_i is less than 2.5°. No model is clearly much better than the other four models. However it is clear that except the SPF model, the fitting errors of the other four classical models are varies a lot for different speakers. For instance, ζ_r of the Thorborg model enjoys the lowest value for L1 and L2, but suffers the highest value for L5. Another problem is that the lowest ζ_r does not bring the lowest ζ_i, which means the model may give the best prediction for the magnitude with the worst for the phase. The magnitude and phase should be fitting separately. With respect to the SPF model, both ζ_r and ζ_i are not the lowest but stand relative low values in all tested loudspeakers.

The models differ in complexity. The simplest model is Leach model with only 2 parameters and the most complicated one is Thorborg model with 5 parameters. Figure 7 shows that the differences between the model accuracies are not too large, and the most complicated model does not give the best fitting results. There seems a compromise between the complexity and the accuracy. The SPF model gives better accuracy with good simplicity for 3 model parameters, just one more than Leach model and one less than Wright model.

Good agreement between model and measured data lend credence to the accuracy of the model, and allows it to be useful in studying the lossy inductance. R'_e, R'_{ES}, L'_{CES} and C'_{MES} predicted by the fitting models were used to get the derived lossy inductance $Z_{LD}(j\omega)$ as

$$Z_{LD}(j\omega) = Z_{meas}(j\omega) - R_e - \left[j\omega C'_{MES} + 1/(j\omega L'_{CES}) + 1/R'_{ES}\right]^{-1}. \quad (13)$$

As examples of the details in the fitting accuracy loudspeakers L1 and L5 are examined in more detail in the following. Figure 8 and Figure 9 delineate the comparisons of the fitted results with the derived lossy inductance of L1 in form of magnitude and phase. Figure 10 and Figure 11 give the comparisons of L5.

It can be concluded from Figure 8 and Figure 10 that: for fitting the magnitude of lossy inductance, all the results increase with frequency, in good correspondence with the derived ones, and the discrepancies between all the models are inconspicuous in low frequency range. Nevertheless,

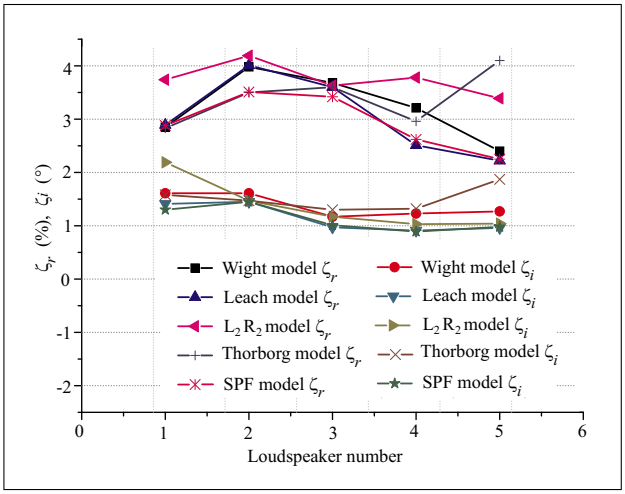

Figure 7. Fitting errors.

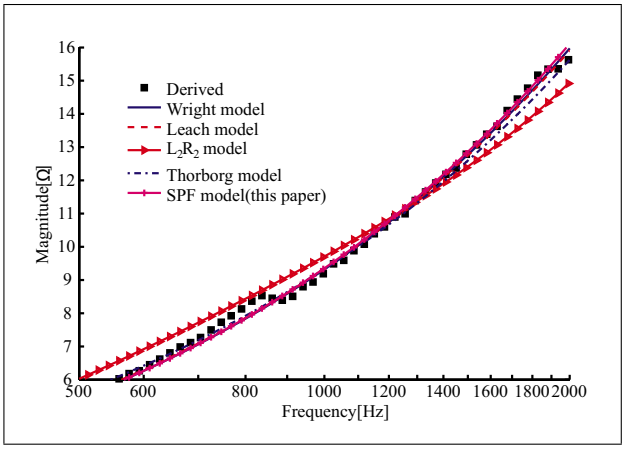

Figure 8. The fitted magnitude of lossy inductance of L1.

there is a significant deviation of the L_2R_2 model when the frequency above 1500 Hz, which confirms the limitation of theL_2R_2 model in term of frequency range.

Equation (1) shows that the phase of Wright model is a power function in angular frequency, depending on the difference between n_i and n_r. Therefore, Figure 9 shows the fitted phase of L1 increases with frequency, but Figure 11 shows the fitted phase of L5 decreases with frequency. According to Equation (2), Figure 9 and Figure 11, the phase of Leach model is independent of frequency. With respect to the L_2R_2 model, both Figure 9 and Figure 11 show that the phase has an opposite shift with the measured one at

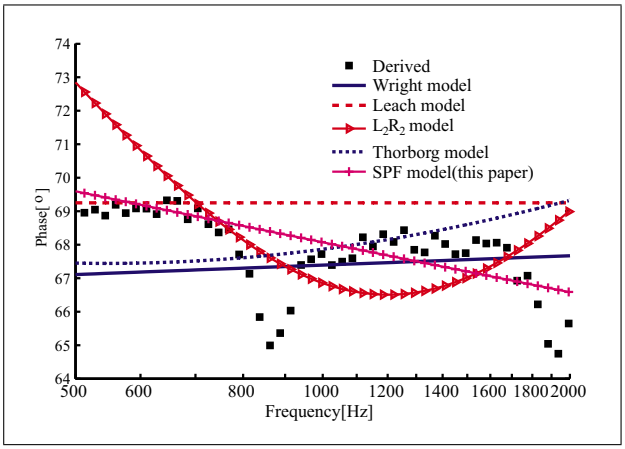

Figure 9. The fitted phase of lossy inductance of L1.

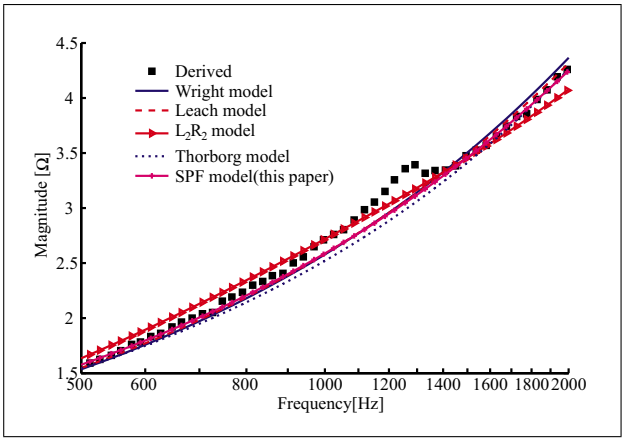

Figure 10. The fitted magnitude of lossy inductance of L5.

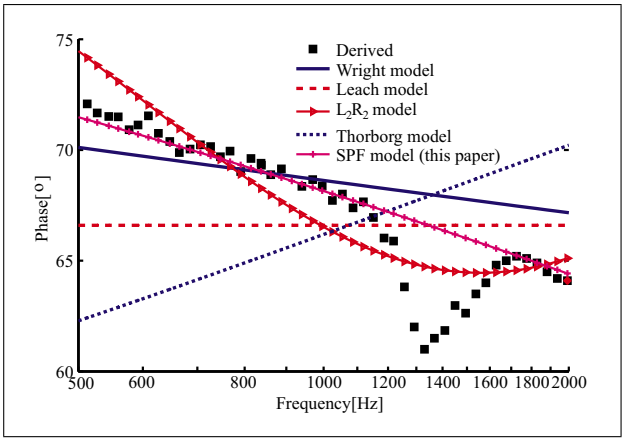

Figure 11. The fitted phase of lossy inductance of L5.

higher frequencies. Although it has the same number of parameters as in SPF model, the accuracy of L_2R_2 is limited. According to Equation (4), the phase of the Thorborg model is really a complicated function in both polynomial functions and power functions of ω, and depends on all the five parameters. Figure 9 and Figure 11 show the fitted phase of Thorborg model increases with frequency, which is in opposite of the measured ones. Since the SPF model fitted the phase as a negative power function of angular frequency, it agrees well with the derived phases.

It should be point out that there are some small ripples at high frequencies (L1 around 850 Hz and 1900 Hz, L5 around 1300 Hz), and it seems that these ripples are due to the resonance modes of the diaphragm [17]or the spider [18].

4. Discussion

As shown in Figure 3 that the phase decreases as a power function in frequency, and reach the asymptotic value at high frequencies. The frequency dependent phase means that the loss of inductance dependents on frequency. At high frequencies, the skin depth in the steel is very small compared with the length of coil, and the eddy currents flow in a thin skin near the surface of the conductor [12].

It should be point out that there are some limitations of the SPF model. In this paper, we just consider the lossy inductance at high frequencies, did not consider the creep effect [10, 11, 19] in loudspeaker suspensions at low frequencies. As modeling the loudspeaker in full range of frequency, the creep models should be added. The simplest creep model is the logarithmic model (LOG) via 2 parameters to predict the compliance of the suspension [19]. Therefore, the loudspeaker linear behaviors can be predicted by at least 8 parameters – 4 basic parameters (R_e, R_{es}, C_{mes} and L_{ces}), at least 2 parameters in the lossy inductance model and at least 2 parameters in the creep model. The optimized function *fminunc* attempts to find a minimum of a scalar function of several parameters, starting at an initial estimate. If the scalar function consist a small number of parameters, some of the characteristics of the fitted data will be lost, and if there are a large number of parameters in the scalar function, the initial values of variables will bias the results and the accuracy is not as stable as before. As an example, putting the with the following parameters $L_0 = 100\,\text{mH}$ and $\lambda = 0.05$ into the electrical impedance instead of L_{ces}, and using the fitted model parameters in Section 3.2.2, then the simulated electrical impedance $Z_{sim}(j\omega)$ can be calculated as

$$L_{ces}^{LOG}(j\omega) = L_0\left[1 - \lambda \log_{10}(j\omega)\right], \tag{14}$$

$$Z_{sim}(j\omega) = R'_e + Z'_L(j\omega) + \left[j\omega C'_{mes} + 1/(j\omega L_{ces}^{LOG}) + 1/R'_{es}\right]^{-1}. \tag{15}$$

Refitting the simulated data without the creep effect included the fitting errors as shown in Table III was obtained. Comparing with Table II, it clearly shows that the fitting errors get worse when there is a mismatch in the mechanical part of the models. However it seems that there is no significant difference between the sensitivity of difference models.

Additionally, the measurements show clear signs of higher order modes in the diaphragm, which is not included in SPF model. These modes will bring significant fitting errors around the mode resonances.

Table III. Refitting errors of simulated electrical impedance.

Model	Wright		Leach		L_2R_2		Thorborg		SPF	
	ζ_r [%]	ζ_i [°]	ζ_r [%]	ζ_i [°]	ζ_r [%]	ζ_i [°]	ζ_r [%]	ζ_i [°]	ζ_r [%]	ζ_i [°]
L1	7.11	4.63	7.44	4.34	7.15	4.67	7.20	4.65	6.92	4.08
L2	7.27	3.98	8.03	3.79	7.19	3.55	7.25	3.67	7.12	3.24
L3	7.67	3.54	7.30	3.22	7.32	3.43	7.98	3.24	7.01	3.09
L4	6.53	2.98	6.77	2.45	6.20	3.02	5.97	3.56	5.11	2.10
L5	5.32	3.40	5.43	2.98	6.34	3.13	6.78	4.05	5.67	2.25

5. Conclusion

By employing two power functions in angular frequency, the separated power function (SPF) model was presented for modeling lossy inductance in moving-coil loudspeakers. SPF model with the other four classical models, Wright model, Leach model, L_2R_2 model and Thorborg model were investigated with the measured electrical impedances of 5 normal loudspeakers. The model accuracy with respect to model complexity was analyzed by fitting the measured impedance curve, and the frequency dependency of the derived lossy inductance phase was discussed. The results show that, for the tested 5 loudspeakers, SPF model can give a good agreement not only with the measured electrical impedance, but also with the derived lossy inductance, especially with the frequency dependent lossy inductance phase. The lossy inductance phase varies with frequency as a negative power function, decreases with frequency in low frequency range, and reaches the asymptotic value at high frequencies.

Acknowledgement

This work has been supported by National Nature Science Foundation of China (Grant No 41374005). The authors wish to thank Acoustic Technology Group, DTU Elektro for providing the experiment instruments and 5 tested loudspeakers.

References

[1] K. Thorborg, C. Futtrup: Electricaldynamic transducers model incorporating semi-inductance and means for shorting AC magnitization. J. Audio Eng. Soc. **59** (2011) 612–627.

[2] J. Vanderkooy: A model of loudspeaker driver impedance incorporating eddy currents in the pole-structure. J. Audio Eng. Soc. **37** (1989) 119–128.

[3] J. R. Wright: An empirical model for loudspeaker motor impedance. J. Audio Eng. Soc. **38** (1990) 749–754.

[4] M. Dodd, W. Klippel, J. O. Brown: Voice-coil impedance as a function of frequency and displacement. 117th AES Convention, San Francisco, USA, October, 2004, 6178.

[5] W. M. Leach: Loudspeaker voice-coil inductance losses: circuit models, parameter estimation, and effect on frequency response. J. Audio Eng. Soc. **50** (2002) 442–450.

[6] W. Klippel: Non-linear large signal behavior of electrodynamic loudspeakers at low frequencies. J. Audio Eng. Soc. **40** (1992) 483–496.

[7] R. B. Mingsian, C. M. Huang: Expert diagnostic system for moving-coil loudspeaker using nonlinear modeling. J. Acoust. Soc. Am. **125** (2009) 819–830.

[8] P. Brunet, B. Shafai: Identification of loudspeakers using fractional derivatives. J. Audio Eng. Soc. **62** (2014) 505–515.

[9] K. Thorborg, D. A. Unruh: Electrical equivalent circuit model for dynamic moving-coil transducers incorporating a semi-inductor. J. Audio Eng. Soc. **56** (2008) 696–709.

[10] K. Thorborg, C. Tinggaard, F. Agerkvist et al.: Frequency dependency of damping and compliance in loudspeaker suspensions. J. Audio Eng. Soc. **58** (2010) 472–486.

[11] K. Thorborg, C. Futtrup: Frequency dependency of the loudspeaker suspensions (a follow up). J. Audio Eng. Soc. **61** (2013) 778–786.

[12] J. R. Bowler, N. Harfield, N. P. Merricks: A theoretical analysis of eddy-current effects in loudspeaker motor. J. Audio Eng. Soc. **48** (2000) 668–678.

[13] I. Schafer, K. Kruger: Modeling of lossy coils using fractional derivatives. J. Phys. D: Appl. Phys. **41** (2008) 045001.

[14] A. M. Concepcion, Y. Chen, B. M. Vinagre et al.: Fractional-order systems and controls: foundamentals and applications. First edition. Springer Press, New York, 2010. 9-34.

[15] T. Pritz: Loss factor peak of viscoelastic materials: magnitude to width relations. Journal of Sound and Vibration **246** (2001) 265–280.

[16] W. Klippel: Large signal identification (LSI). http://d.sangjinmedia.co.kr/ upload/ 02%20Klippel/ 01%20R&D20System/ 03%20Software%20Module/ 02%20LSI/ S1-LSI.pdf.

[17] N. Quaegebeur, A. Chaigne: Nonlinear vibrations of loudspeaker-like structures. Journal of Sound and Vibration **309** (2008) 178–196.

[18] H. David, G. Gary: Finite element modeling of a loudspeaker. Part 1: Theory and validation. 119thAES Convention, New York, USA, 2005, 6582.

[19] F. Agerkvist, K. Thorborg, C. Tinggaard: A study of the creep effect in loudspeaker suspension. 125th AES Convention, San Francisco, USA, October, 2008, 7561.